

Metallicity in the Galactic Center: The Arches cluster

Francisco Najarro¹, Donald F. Figer², D. John Hillier³, Rolf P. Kudritzki⁴

najarro@damir.iem.csic.es

ABSTRACT

We present a quantitative spectral analysis of five very massive stars in the Arches cluster, located near the Galactic center, to determine stellar parameters, stellar wind properties and, most importantly, metallicity content. The analysis uses a new technique, presented here for the first time, and uses line-blanketed NLTE wind/atmosphere models fit to high-resolution near-infrared spectra of late-type nitrogen-rich Wolf-Rayet stars and OfI⁺ stars in the cluster. It relies on the fact that massive stars reach a maximum nitrogen abundance that is related to initial metallicity when they are in the WNL phase. We determine the present-day nitrogen abundance of the WNL stars in the Arches cluster to be 1.6% (mass fraction) and constrain the stellar metallicity in the cluster to be solar. This result is invariant to assumptions about the mass-luminosity relationship, the mass-loss rates, and rotation speeds. In addition, from this analysis, we find the age of the Arches cluster to be 2-2.5 *Myr*, assuming coeval formation.

Subject headings: Galaxy: abundances – stars: abundances – stars: Wolf-Rayet – infrared: stars – Galaxy: center

1. Introduction

The determination of metal abundances as a function of time and Galactic location (e.g. disk, bulge and halo) provides crucial information for understanding the formation and

¹Instituto de Estructura de la Materia, CSIC, Serrano 121, 29006 Madrid, Spain

²Space Telescope Science Institute, 3700 San Martin Drive, Baltimore, MD 21218

³Department of Physics and Astronomy, University of Pittsburgh, 3941 O'Hara Street, Pittsburgh, PA 15260

⁴Institute for Astronomy, University of Hawaii, 2680 Woodlawn Drive, Honolulu, HI 96822

evolution of our Galaxy. Such studies are required to constrain the influence of the initial mass function, star formation rates, infall and outflow rates and stellar yields in the galactic models. The metal content appears depleted in the halo and ancient populations of globular clusters and displays a roughly solar value in the metal-rich bulge (Frogel et al. 1999; Feltzing & Gilmore 2000). So far, models have predicted the presence of a metallicity gradient in the Galactic disk with lower metallicity at increasing galactocentric distances. This result has been confirmed by several studies using different diagnostic tools. Good agreement has been found among results from HII regions (Afflerbach et al. 1997), planetary nebulae (Maciel & Quireza 1999), nearby cool stars in the galactic disk (Fuhrmann 1998) and early stars (B-type) between 2.5 and 18kpc (Rolleston et al. 2000; Smartt et al. 2001).

Whether the Milky Way follows the trends observed in other spirals (Urbaneja et al. 2004; Kennicutt et al. 2003) and reaches its highest metallicity value in its center or if on the contrary our Galactic center is unrelated to the starforming galactic disk is still a source of controversy. Based on measurements of the gas-phase, Shields & Ferland (1994) obtained twice solar metallicity from argon and nitrogen emission lines, while a solar abundance was derived for neon. Further, Maeda et al. (2000) recently obtained four times solar abundance by fitting the X-ray local emission around Sgr A East. On the other hand, for the cool stars, and based on LTE-differential analysis with other cool supergiants, Carr et al. (2000) and Ramirez et al. (1997, 1999, 2000) have obtained strong indications for a solar Fe abundance. It is therefore crucial to obtain metallicity estimates from objects providing direct diagnostics, such as hot stars, and confront them with those from the cool-star and gas-phase analyses. Spectroscopic studies of photospheres and winds of massive hot stars are ideal tracers of metal abundances because they provide the most recent information about the natal clouds and environments where these objects formed.

The Galactic center is clearly a unique environment in the Galaxy. It hosts three dense and massive star clusters that have recently formed in the inner 50 pc. The Arches Cluster (Figer et al. 1999, 2002) is the youngest and densest cluster at the Galactic center containing thousands of stars, including at least 160 O stars and around 10 WNLs (WN stars still showing H at their surface, Chiosi & Maeder 1986). The cluster is very young (≤ 2.5 Myr), and the only emission line stars present are WNLs and OIf⁺ having infrared spectra dominated by H, He I, He II, N III lines. Some have weak C III/IV lines. The absence of late B-supergiants and LBVs prevents one from obtaining direct estimates of the important α -elements vs. Fe metallicity ratio via the Fe II, Si II & Mg II lines, as can be done for older clusters like the Quintuplet (Najarro et al. 2004) or the Central parsec cluster. Being the youngest cluster at the Galactic center, any hint about its metallicity would constitute our “last-minute” picture of chemical enrichment of the central region in the Milky Way.

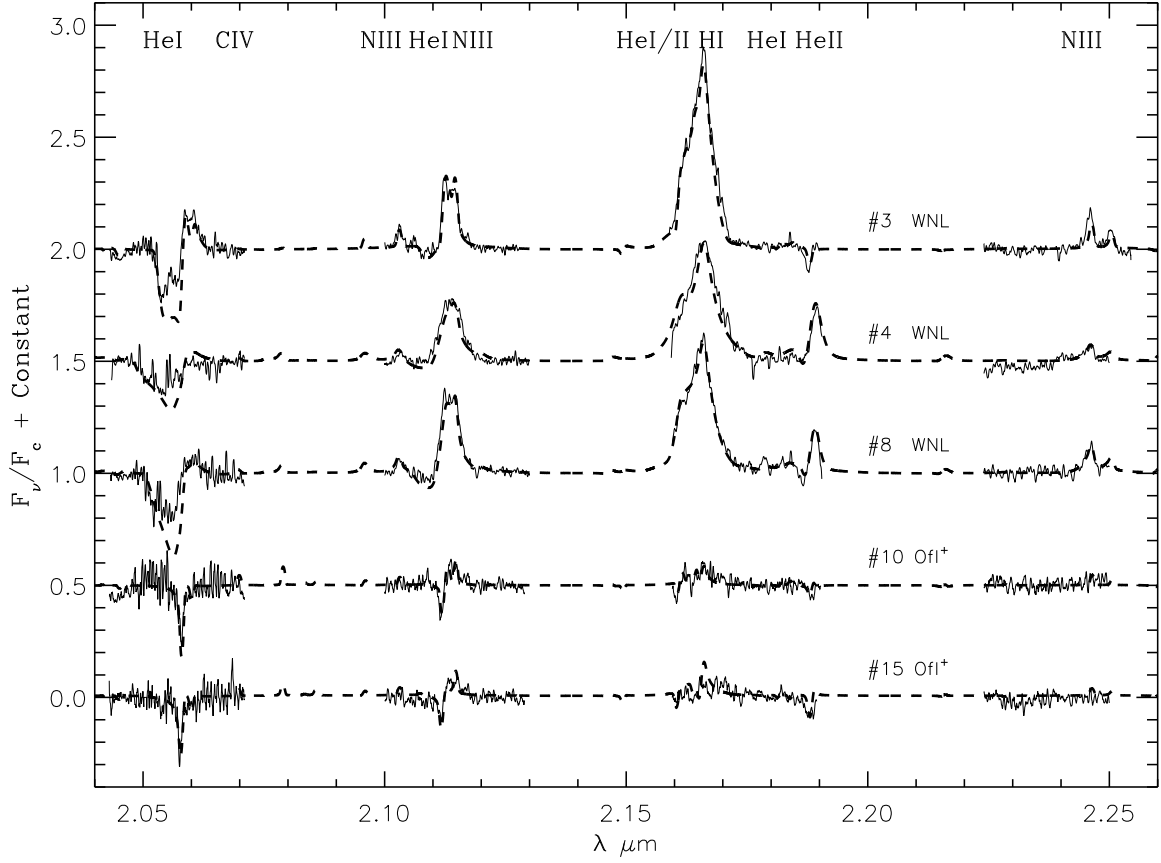


Fig. 1.— Observed spectra (*solid*) and model fits (*dashed*) for the three WNL and two OfI⁺ Arches stars. The WNL stars generally have strong He I lines at 2.058 μm , 2.112 μm , 2.166 μm , and 2.189 μm , and weaker N III lines at 2.104 μm , 2.115 μm , 2.248 μm , and 2.250 μm . H I contributes to the 2.166 μm line. The OfI⁺ stars have He I absorption lines at 2.058 μm and 2.112 μm , N III emission lines at 2.115 μm , and, perhaps, weak H I emission at 2.116 μm . Model parameters are listed in Table 1 and objects are given according to Figer et al. (2002)

In this paper, we perform quantitative infrared spectroscopy of the Arches cluster and provide a robust method to derive metallicity in WNL stars using their surface nitrogen abundances and the properties of stellar evolution models.

2. Observations and Data Reduction

The observations and data reduction are described in Figer et al. (2002), and a brief summary is provided below. The spectroscopic observations were obtained on July 4, 1999, using NIRSPEC, the facility near-infrared spectrograph, on the Keck II telescope (McLean et al. 1998), in high resolution mode, covering K -band wavelengths (1.98 μm to 2.28 μm). The long slit (24") was positioned in a north-south orientation on the sky, and a slit scan covering a 24" \times 14" rectangular region centered on the Arches cluster was made by offsetting the telescope by a fraction of a slit width to the west between successive exposures. The resolving power was $R \sim 23,300$ ($=\lambda/\Delta\lambda_{\text{FWHM}}$), using the 3-pixel wide slit, as measured from unresolved arc lamp lines.

Quintuplet Star #3 (hereafter “Q3”), which is featureless in this spectral region (Figer et al. 1998, Figure 1), was observed as a telluric standard (Moneti et al. 1994). Arc lamps were observed to set the wavelength scale. The spectra were reduced using IDL and IRAF routines.

The data were bias and background subtracted, flat fielded, corrected for bad pixels, and transformed onto a rectified grid of data points spanning linear scales in the spatial and wavelength directions.

In addition we make use of HST/NICMOS narrow band photometry from Figer et al. (2002), which provides equivalent width measurements of $P\alpha$.

3. Models & Discussion

To model the massive Arches stars and estimate their physical parameters, we have used the iterative, non-LTE line blanketing method presented by Hillier & Miller (1998). The code solves the radiative transfer equation in the co-moving frame for the expanding atmospheres of early-type stars in spherical geometry, subject to the constraints of statistical and radiative equilibrium. Steady state is assumed, and the density structure is set by the mass-loss rate and the velocity field via the equation of continuity. We allow for the presence of clumping via a clumping law characterized by a volume filling factor $f(r)$. The model is then prescribed by the stellar radius, R_* , the stellar luminosity, L_* , the mass-loss rate

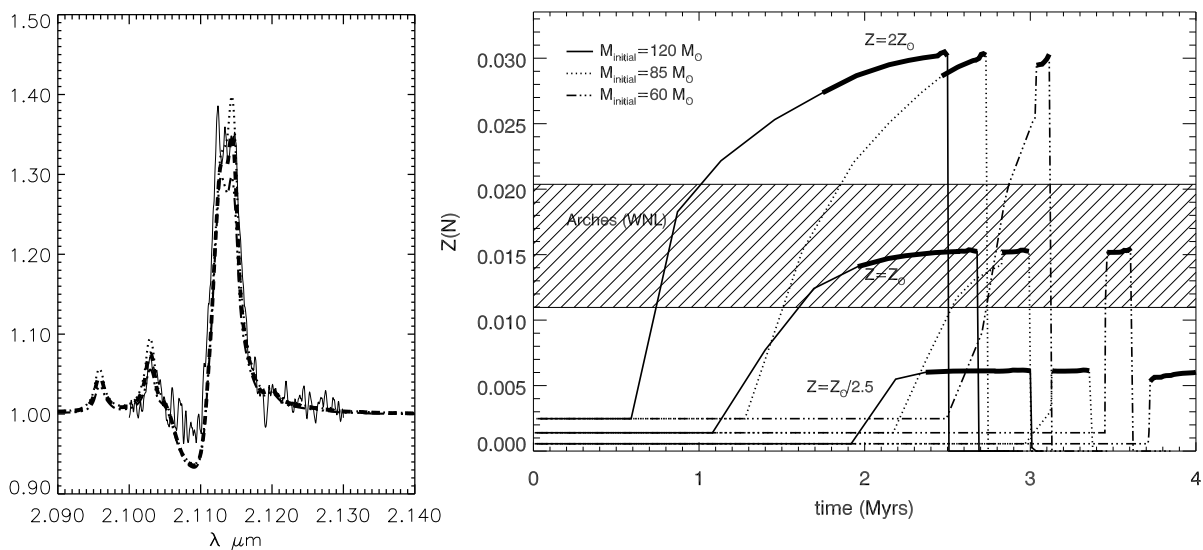


Fig. 2.— *Left.* Leverage of error estimates on N abundance. Shown is observed 2.10-2.13 μm region (solid) together with current best fit (dashed) and 30% enhanced (dotted) and 30% depleted (dashed-dotted) nitrogen mass fractions. The N III 2.247-2.251 μm doublet (not shown here) displays even higher sensitivity. *Right.* Plot of nitrogen mass abundance versus time using Geneva models (Schaller et al. 1992; Charbonnel et al. 1993) for stars with initial masses of 60, 85, and 120 M_{\odot} , and for initial metallicities of $Z_{\odot}/2.5$, Z_{\odot} , and $2Z_{\odot}$; we assume canonical mass-loss rates and no rotation. The bold lines correspond to the WNL stellar evolution phase, when the nitrogen mass surface abundance reaches its maximum. The derived nitrogen mass abundances and corresponding errors for the Arches WNLs are cross-hatched. The measurements require solar metallicity and an age of 2-2.5 *Myr*.

\dot{M} , the velocity field, $v(r)$, the volume filling factor, f , and the abundances of the elements considered. Hillier & Miller (1998, 1999) present a detailed discussion of the code. For the present analysis we have assumed the atmosphere to be composed of H, He, C, N, O, Si and Fe.

Observational constraints are provided by the K-Band spectra of the stars (see Figure 1) and the narrow band HST/NICMOS photometry (filters F_{F110W} , F_{F160W} & F_{F205W}) and $P\alpha$ equivalent width (filters F_{F187N} & F_{F190N}). Object identifications are given according to Figer et al. (2002).

The reduced spectra and model fits are shown in Figure 1. The top three spectra correspond to some of the most luminous stars in the cluster. As described in Figer et al. (2002), these are nitrogen-rich Wolf-Rayet stars with thick and fast winds. The bottom two spectra in the figure correspond to slightly less evolved stars with the characteristic morphology of OIf⁺ stars (e.g. HD151804, Crowther & Bohannan 1997). The main diagnostic H and He lines in the observed K band portions (see Figure 1) are Br γ , the He I lines at 2.058 μm , 2.060 μm , 2.112/3 μm , 2.160-66 μm and 2.181 μm and the He II lines at 2.165 μm , 2.189 μm . The main carbon lines which may be used to place upper limits on the carbon abundance are C IV 2.070 μm and C III 8-7 at 2.114 μm . Of concern are the N III 8-7 lines at 2.103 μm and 2.115 μm as well as the N III 5p²P–5s²S doublet at 2.247 μm and 2.251 μm . Figer, McLean, & Najarro (1997) showed that these N III lines appear only for a narrow range of temperatures and wind densities, which occur in the WN9h (WNL) stage. The fairly distinct nature and energies of the multiplets involved in each of both N III line sets provide strong constraints for the determination of the nitrogen abundance. Thus, at the S/N of our spectra, our models show that the WNLs N III lines can easily track relative changes as low as 20% in the nitrogen abundance, and a 30% error should be regarded as a safe estimate, as shown in Figure 2-*left*.

Individual stellar parameters of the WNL stars (objects #3,#4 & #8) are listed in Table 1, together with those derived for two OIf⁺ stars (#10 & #15) in the cluster. It is important to note that given the extreme sensitivity of the He I and He II line profiles in this parameter domain to changes in effective temperature, we estimate our errors to be below 1000 K. For the WNLs, the clumping factor is basically determined by the red emission wing of Br γ , while V_∞ is set by the He I 2.058 μm line. For the OIf⁺ stars, we investigated the effects of varying both the clumping factor and the terminal velocity. Only an upper limit is obtained for the latter from the shape of the Br γ -He complex at 2.16 μm , while there was no unique solution for f . Therefore we adopted $f=0.1$, which is roughly the average value found for the WNLs. For all objects, the relative strength between the H and He I lines is used to derive the He/H ratio while their absolute strengths provide \dot{M} . The stellar parameters

displayed in Table 1 (\dot{M} , He and N abundance) reflect the striking difference in morphology between the observed WNL and OIf⁺ spectra. Of particular importance is the roughly same surface abundance fraction of N, $Z(N)$, obtained for all three WNL objects ($\sim 1.6\%$) well above the upper limit found for the OIf⁺ stars ($\sim 0.6\%$). WNL stars do not exhibit any primary diagnostic line in their K-Band spectra to estimate metallicity. However, the crucial rôle of $Z(N)$ in determining metallicity from WNL stars can be immediately anticipated if we make use of the stellar evolution models for massive stars.

According to the evolutionary models by Schaller et al. (1992) and Charbonnel et al. (1993), a star entering the WNL phase still shows H at its surface together with strong enhancement of helium and nitrogen and strong depletion of carbon and oxygen as expected from processed CNO material. Further, once a massive star reaches this phase, it maintains a nearly constant $Z(N)$ value throughout this period, and the amount achieved essentially depends only linearly on the original metallicity (see Figure 2-*right*). Namely, the maximum $Z(N)$ in the WNL phase is set by the initial content of CNO (sum of C, N and O mass fractions) present in the natal cloud. However, since we expect the CNO abundance in the natal cloud to scale as the rest of metals, the nitrogen surface abundance must trace the metallicity of the cluster. Further, this value is basically unaffected by the mass-loss rate assumed and the presence of stellar rotation during evolution (Meynet & Maeder 2004). Hence, once we clearly identify a star to be on the WNL evolutionary phase, we may confidently use its N surface abundance fraction to estimate metallicity. The He/H ratio, the upper limit on the very depleted carbon abundance and the T_{eff} and \dot{M} values indicate that this is the case for objects #3, #4 & #8. The derived $Z(N)$ ($\sim 1.6\%$) is the one expected for **solar** metallicity from the evolutionary models. Due to the linear behavior of $Z(N)$ with metallicity, we make use of the uncertainties in the N abundance estimate to obtain an error of roughly 30% for the metallicity (see Figure 2-*left*). The reliability of our method is demonstrated in Figure 2-*right*, where we display the nitrogen mass fraction as a function of time for stars with initial masses of 60, 85, and 120 M_{\odot} , and metallicities equivalent to 2, 1, and 0.4 times solar, assuming the canonical mass-loss rates (Schaller et al. 1992). The cross-hatched region represents our estimates including the above quoted errors of the nitrogen mass fraction for the Arches WNLs. To test the validity of the nitrogen abundance method to trace metallicity, we may compare our results with previous abundance estimates for these objects in regions of different metallicity. Indeed, Crowther (2000) found that the nitrogen surface abundance value reached during the WNL phase in the SMC (0.3%) reproduced very well the observed spectra of SK-41 while, Crowther, Hillier, & Smith (1995) found surface abundances corresponding to solar metallicity in their analysis of galactic WNL stars.

Another important direct result from Figure 2 and Table 1 is a tight estimate for the masses and ages of the objects. The luminosities of #4 & #8 are consistent with initial

masses of $\sim 120 M_{\odot}$ for these WNL stars while the luminosity of #15 seems to be consistent with masses $70\text{-}90 M_{\odot}$ for the O stars. Assuming these masses, equal initial abundances, and coeval formation, one finds that both the WNL and O stars require solar metallicity and an age of $2\text{-}2.5 Myr$. Current luminosities of #3 and #10 can be interpreted in terms of the effects of rotation on the evolution of massive stars. New evolutionary models for massive stars including rotation (Meynet & Maeder 2004) show that the WNL phase is reached much faster for those objects with high initial rotational velocities. Once the star reaches the WNL phase, its luminosity starts to decrease. Thus, for a given initial ZAMS mass, a scatter in the initial rotational velocity will result in a range of current luminosity.

If our assumption of coeval star formation is correct, the OIf⁺ star #10 with current high luminosity, but which is less evolved than the WNLs, should have had a much lower initial velocity than the rest of the WNLs (see tracks by Meynet & Maeder 2004). While this assumption can not be proved, as we have no way to estimate the current rotational velocity of the WNLs, a high present rotational velocity for the OIf star #10 would definitely rule out such a scenario. We use our models to find a consistent maximum rotational velocity of $v \sin i < 75 \text{ km/s}$ for #10 from the narrow He I $2.058 \mu\text{m}$ absorption line (see Fig. 1). Likewise, the low current luminosity of the WNL star #3 would be consistent with a slightly lower ZAMS mass than #4 and #8 and a higher initial rotational velocity (as shown in the evolutionary tracks by Meynet & Maeder 2004).

Our result of solar metallicity runs counter to the trend in the disk (Rolleston et. al. 2000; Smartt et. al. 2001) but is consistent with the findings from cool star studies (Carr et al. 2000; Ramirez et al. 1997, 1999, 2000). This may imply that the ISM in the disk does not extend inward to the GC, or that the GC stars are forming out of an ISM that has an enrichment history that is distinctly different from that in the disk. Our result is more consistent with the values found for the bulge (Frogel et al. 1999; Feltzing & Gilmore 2000). Further results for other GC regions, like the Central cluster or the Quintuplet cluster (Najarro et al. 2004) are needed. In a forthcoming paper we will investigate the wind properties of a large sample (~ 20 objects) of WNL and OIf stars in the Arches cluster.

We thank George Meynet and Andre Maeder for useful discussions. F. N. acknowledges grants AYA2003-02785-E and ESP2002-01627.

REFERENCES

Afflerbach, A., Churchwell, E. B. & Werner, M.W., 1997, ApJ, 478, 190

- Carr, J.S., Sellgren, K. & Balachandran, S.C. 2000, *ApJ*, 530, 307
- Charbonnel, C., Meynet, G., Maeder, A., Schaller, G., & Schaerer, D. 1993, *A&AS*, 101, 415
- Chiosi, C. & Maeder, A. 1986, *ARA&A*, 24, 329
- Crowther, P. A. & Bohannan, B. 1997, *A&A*, 317, 532
- Crowther, P. A. 2000, *A&A*, 356, 191
- Crowther, P. A., Hillier, D. J., & Smith, L. J. 1995, *A&A*, 293, 403
- Feltzing, S., & Gilmore, G. 2000, *A&A*, 355, 949
- Figer, D. F., Najarro, F., Morris, M., McLean, I. S., Geballe, T. R., Ghez, A. M., & Langer, N. 1998, *ApJ*, 506, 384
- Figer, D. F., McLean, I. S., & Najarro, F. 1997, *ApJ*, 486, 420
- Figer, D. F., Morris, M., Geballe, T. R., Rich, R. M., Serabyn, E., McLean, I. S., Puetter, R. C., & Yahil, A. 1999b, *ApJ*, 525, 759
- Figer, D. F., et al. 2002, *ApJ*, 581, 258
- Frogel, J.A., Tiede, G.P., & Kuchinski, L.E. 1999, *AJ*, 117, 2296
- Fuhrmann, K., 1998, *A&A*, 338, 161
- Hillier, D. J. & Miller, D. L. 1998, *ApJ*, 496, 407
- Hillier, D. J. & Miller, D. L. 1999, *ApJ*, 519, 354
- Kennicutt, R.C., Bresolin, F., Garnett, D.R. 2003, *ApJ*, 591, 544
- Maeda, Y., et. al., 2002, *ApJ*, 570, 671
- Maciel, W.J., & Quireza, C. 1999, *A&A*, 345, 629
- McLean et al. 1998, *SPIE Vol. 3354*, 566
- Meynet, G., Maeder, A., Schaller, G., Schaerer, D., & Charbonnel, C. 1994, *A&A Supp.*, 103, 97
- Meynet, G.,&— Maeder, A., 2004, *A&A*, 404, 975
- Moneti, A., Glass, I. S. & Moorwood, A. F. M. 1994, *MNRAS*, 268, 194

- Najarro, F., Figer, D.F., et. al., (in preparation)
- Ramirez, S.V., Carr, J.S., Balachandran, S., Blum, R., & Terndrup, D.M. 1997, in IAU Symp. 184, The Central Regions of the Galaxy and Galaxies, ed. Y. Sofue (Dordrecht: Kluwer), 28
- Ramirez, S.V., Sellgren, K., Carr, J.S., Balachandran, S., Blum, R., & Terndrup, D.M. 1999, ASP Conf. Ser. 186: The Central Parsecs of the Galaxy
- Ramirez, S.V., Sellgren, K., Carr, J.S., Balachandran, S., Blum, R., Terndrup, D.M., & Steed, A., 2000, ApJ, 537,205
- Rolleston, W.R., Smartt, S.J., Dufton, P.L., & Ryans, R.S.I., 2000, A&A, 363, 537
- Schaller, G., Schaerer, D., Meynet, G., & Maeder, A. 1992, A&AS, 96, 269
- Shields, J.C., & Ferland, G.J., 1994, ApJ, 430, 236
- Smartt, S.J., Venn, K.A., Dufton, P.L., Lennon, D.J., Rolleston, W.R., & Keenan, F.P., 2001, A&A, 367, 86
- Urbaneja, M.A., Herrero, A., Bresolin, F., Kudritzki, R.P., Gieren, W., Puls, J., Przybilla, N., Najarro, F., Pietrzynski, G., 2004, ApJ, submitted

Table 1. WNL and O stars in the Arches Cluster

Parameter	#3	#4	#8	#10	#15
$R_*(R_\odot)$	43.5	39	48	48	29
$L_*(10^5 L_\odot)$	10.3	16.5	18.5	18.5	5.85
$T_{\text{eff}}(10^4\text{K})$	2.79	3.32	3.09	3.07	2.95
He/H	0.50	0.57	0.67	0.33	0.33
Z(He)	0.65	0.68	0.71	0.56	0.56
Z(N)	1.7	1.4	1.6	0.6:	0.6:
Z(C)	0.02:	0.03:	0.02:	0.08:	0.15:
$\dot{M}(10^{-6} M_\odot \text{ yr}^{-1})$	21.5	32.5	45.0	4.3	9.11
$V_\infty(\text{km s}^{-1})$	840	1400	1100	1000:	1000:
Clumping factor f	0.1	0.15	0.08	0.1	0.1
$\eta = \dot{M} V_\infty / (L_*/c)$	0.72	1.35	1.32	0.11	0.75
Log Q_{H^+}	49.4	49.9	49.9	49.8	49.2
Log Q_{He^+}	47.3	48.6	48.5	48.4	47.3

Note. — Object identifiers after Figer et al. (2002). Upper limits are quoted as (:). He/H is ratio by number and other abundances are mass fractions. η is the performance number and Q is the ionizing photons rate in photons/s.